Journal of Applied Polymer Science

Potential Role of Nanofillers as Compatibilizers in Immiscible PLA/LDPE Blends

Domagoj Vrsaljko, Dejan Macut, Vera Kovačević
Faculty of Chemical Engineering and Technology, University of Zagreb, HR-10000 Zagreb, Croatia
Correspondence to: D. Vrsaljko (E-mail: dvrsal@fkit.hr)

ABSTRACT: This article describes the use of commercial silica (SiO_2) and calcium carbonate ($CaCO_3$) nanofillers as compatibilizers in immiscible polylactide/low-density polyethylene (PLA/LDPE) blends. The general aim of the study was to investigate the possibilities of replacing standard commodity plastics such as LDPE based on non-renewable mineral oil resources with the biodegradable renewable polymer PLA in compatibilized PLA/LDPE blends for use in the packaging industry. The calculations of the minimal interfacial energy and optimal wetting abilities indicated that SiO_2 filler was a better potential compatibilizer than $CaCO_3$ for a given PLA/LDPE blend. This was due to its preferential localization at the interface. The significantly improved morphology of the ternary PLA/LDPE/SiO_2 blend was found to present an increased strength, toughness, and crystallinity. © 2014 Wiley Periodicals, Inc. J. Appl. Polym. Sci. **2015**, *132*, 41414.

KEYWORDS: blends; compatibilization; Mechanical properties; surfaces and interfaces

Received 20 June 2014; accepted 13 August 2014
DOI: 10.1002/app.41414

INTRODUCTION

The challenges of environmental, economic, and safety issues have forced scientists working with packaging products, as well as producers, to replace polymers based on petrochemicals with biodegradable polymers, or with nanocomposites,[1] free from toxic components, that will biodegrade into natural products.[2,3] The most important biodegradable polymers include aliphatic polyesters, such as polylactide (PLA),[4] which are so-called eco-friendly materials with great potential for development.[5] PLA represents one of several polymers that could reduce societal problems associated with waste management.[6] During the past decade, PLA has been intensively investigated,[7–9] as have its applications and market.[5]

PLA represents an alternative to petrochemical plastics in various applications, including the paper, fibril, film, and packaging industries.[10,11] Thanks to its good mechanical properties and physical characteristics, PLA is interesting especially for the food industry.[12–14] Its main problem is its brittleness at room temperature which presents its general disadvantage in application.[15] Numerous studies have thus been devoted to biopolymers with the aim of creating combinations with standard polyolefines to fulfill application conditions.[15,16] Also, studies have been conducted on integrating inorganic nanofillers,[2,17–19] with large active surface areas, to improve mechanical properties, resistance to heat, as well as dimensional and thermal stability of the final composite, as a consequence of filler interactions with the matrix. In our earlier investigations, we suggested the possibilities of using nanofillers as reinforcing agents in composites and as compatibilizers in immiscible blends.[20–22]

This article describes an investigation of the effects of blending PLA with a standard polyolefin, that is, low density polyethylene (LDPE), as well as what impact the incorporation of selected commercial nanofillers, either silica or calcium carbonate, would have on the interface and related morphology, mechanical, and thermal properties. The chosen fillers, that is, nanosilica (SiO_2),[17] or nano-calcium carbonate ($CaCO_3$),[14] are commonly used in such applications. The interactions of nanofillers in a polymer blend and their preferential localization at the interface could significantly enhance the properties.[23,24]

EXPERIMENTAL

Materials

The compositions of the initial polymer blends are given in Table I. Unfilled initial blend samples were prepared in a Brabender mixer with a heating time of 5 min, a temperature of 190°C and a screw speed of 60 rpm. For the testing of mechanical and thermal properties, film samples were prepared in a Dake hydraulic press, at 190°C with a preheating time of 3–4 min and heating under pressure for 5 min. The same procedure was used for the preparation of the blends filled with the same concentration (5 wt %) of commercial nanofillers, that is, SiO_2 and $CaCO_3$ (Table II).

Table I. Compositions of the Initial PLA/LDPE Blends

PLA (wt %)	LDPE (wt %)
100	0
90	10
80	20
60	40
50	50
40	60
30	70
20	80
10	90
0	100

Characterization

Surface investigations of the fillers and the blend samples were done on a DataPhysics OCA 20 goniometer by measuring contact angles with three test liquids (water, formamide, and diiodomethane) with known surface energy values.[25] Contact angle measurements represent a valid method for determining the surface energy of solid materials.[26] Contact angles were measured by the sessile drop method, that is, by placing a drop of the test liquid on the sample surface, with at least six repeated measurements to ensure the reproducibility of the measured data. Samples of SiO_2 and $CaCO_3$ fillers were prepared by pressing the powder at room temperature. The samples of the pure PLA and LDPE polymers and their unfilled and filled blends were prepared by melt pressing at 190°C followed by cooling at 25°C.[18]

The surface energies of the PLA and LDPE polymers, as well as of the SiO_2 and $CaCO_3$ fillers, were calculated from the contact angle data using the Wu method[27] [eq. (1)], as well as the interfacial energy [eq. (2)]:

$$\gamma_{lv}(1+\cos\theta)=\frac{4\gamma_s^d\gamma_{lv}^d}{\gamma_s^d+\gamma_{lv}^d}+\frac{4\gamma_s^p\gamma_{lv}^p}{\gamma_s^p+\gamma_{lv}^p} \quad (1)$$

$$\gamma_{mf}=\gamma_m+\gamma_f-\frac{4\gamma_m^d\gamma_f^d}{\gamma_m^d+\gamma_f^d}-\frac{4\gamma_m^p\gamma_f^p}{\gamma_m^p+\gamma_f^p} \quad (2)$$

where γ^d is the dispersive and γ^p the polar component of the surface free energy ($\gamma=\gamma^d+\gamma^p$); γ_{lv} and γ_s are the surface free energies of the liquid and solid, respectively, θ is the contact angle, and the suffixes m and f, respectively, stand for matrix and filler. The Wu equation is recommended for systems containing both materials with high surface energies, such as fillers, and low surface energies, such as polymers.

Mechanical properties were measured on a Zwick 1445 tensile testing apparatus, with the following test conditions: a speed of 10 mm/min and a gauge length of 50 mm. The results were averages of tests of five specimens of each sample. Furthermore, the impact strength was measured by Izod testing according to ISO 180-2000.

A VEGA 3 Tescan and FE-SEM, Mira/LMU Tescan scanning electron microscopes were used as the primary technique to determine the morphology of the unfilled and filled blends.

The crystallinity of PLA and its blends was determined by DSC on a Mettler Toledo DSC 823e with an inert stream of nitrogen flowing at 50 ml/min according to a protocol[19] of two heating cycles with a heating speed of 10°C/min and one cooling cycle with the cooling rate of 10°C/min as follows:

First heating cycle from −90°C to 200°C; 200°C, 3 min (stabilization);

Cooling from 200°C to −90°C; −90°C, 3 min (stabilization);

Second heating cycle from −90°C to 200°C; 200°C, 1 min (stabilization); cooling from 200°C to 25°C.

The crystallinity of PLA was determined based on the regime of heating and cooling defined below.[28] The thermal history of the sample was erased by the first heating. From the second heating scans,[28] the glass transition temperature (T_g), cold crystallization (T_{cc}), and melting temperature (T_m), as well as enthalpies (ΔH_{cc}, ΔH_m) were determined.

The degree of crystallinity of the initial PLA sample, χ_c, was calculated using the common two-phase approximation: $\chi_c=\Delta H_m/\Delta H_m^0$, where ΔH_m is the measured enthalpy of melting and ΔH_m^0 is the melting enthalpy of 100% crystalline polymer (~93 J/g for PLA).[17,29–31] The crystalline structure of the composite and blends was calculated using eq. (3)[32,33]:

$$\chi_c=\Delta H_{m\mathrm{PLA}}/\Delta H_{m\mathrm{PLA}}^0 w_f \cdot 100\% \quad (3)$$

where χ_c is the degree of crystallinity of the PLA matrix, $\Delta H_{m\mathrm{PLA}}$ is the melting enthalpy of PLA in the composite, blend

Table II. Characteristics of the Commercial Fillers and Polymers

	Characteristics					
Samples	BET (m^2/g)	Poured density (g/L)	Pretreatment	T_g (°C)	T_m (°C)	Density (g/cm^3)
SiO_2[a]	125-175	60	Methacrylsilane			
$CaCO_3$[b]	8	200-600	-			
PLA[c]				55-60	155-170	
LDPE[d]						0.923

[a] Evonik Industries AG (Aerosil® R711).
[b] Schaefer Kalk GmbH & Co. KG (Precarb 400).
[c] NatureWorks LLC (Ingeo™ Biopolymer 3251D).
[d] The Dow Chemical Company (DOW™ LDPE 780E).

Table III. Surface and Interface Characteristics of the Initial Polymers, the Fillers, and the Blend Samples

	Surface (mJ/m^2)			Interface (mJ/m^2)						
				$\gamma_{interface}$[b]		W[c]		S[d]		Filler localization
Sample	γ^d [a]	γ^p	γ	$\gamma_{f/PLA}$	$\gamma_{f/LDPE}$	$W_{f/PLA}$	$W_{f/LDPE}$	$S_{f/PLA}$	$S_{f/LDPE}$	ωa[e]
Polymer										
PLA	25.1	6.6	31.8							
LDPE	24.6	9.2	33.8							
Filler										
SiO_2	45.5	7.8	53.3							
$CaCO_3$	37.1	32.5	69.6							
Blend										
PLA/LDPE				0.42		65.1		−2.47		
PLA/LDPE/SiO_2				5.97	6.34	79.1	80.7	15.6	13.1	0.88 interf.[f]
PLA/LDPE/$CaCO_3$				19.3	15.5	81.9	87.8	18.4	20.22	−9.01 LDPE[g]

[a] Surface energy: eq. (1).
[b] Interface energy: eq. (2).
[c] Work of adhesion: $W_{mf}=\gamma_f+\gamma_m-\gamma_{mf}$ (m = matrix, f = filler).
[d] Coefficient of wetting: $S_{mf}=\gamma_f-\gamma_m-\gamma_{mf}$.[36]
[e] Filler localization in blend: eq. (4).[37]
[f] The SiO_2 filler was situated at the interface in PLA/LDPE blend.
[g] The $CaCO_3$ filler was situated in the LDPE phase.

and/or filled blend, ΔH_m^0 is the melting enthalpy of the completely crystalline PLA (93.7 J/g),[17,29,30] and w_f is the mass percentage of PLA, or expressed as $(1-m_f)$ with m_f as weight percentage of the other component except PLA,[19] or expressed as f, that is, the mass of the component in question.[34]

Sequential heating and cooling were provided to verify the changes in glass transition, T_g, and to follow the protocol that enables to obtain cold-crystallized samples through heating from the glassy state.[28] The glass transition temperature, T_g, was measured as the midpoint on the inflection of the heat capacity, whereas the cold crystallization temperature, T_{cc}, and melting temperature, T_m, were determined from the peaks of the related endothermic and exothermic maxima.[3,35]

RESULTS AND DISCUSSION

Surface and Interface

Table III lists the surface and interface characteristics of the samples containing commercial SiO_2 and $CaCO_3$ fillers, PLA and LDPE polymers as well as the prepared unfilled and filled blends. The relatively low interfacial energy, $\gamma_{interface}$, between PLA and LDPE was assigned to the affinity for mixing, but the negative value of the wetting coefficient, S, was an indication of debonding at the interface in the immiscible blends (Table III) and thus of the necessity of compatibilization by addition of a nanofiller. The selectivity of the filler of being localized in the polymer phases or migrating to the interface can be calculated using various models based on criteria that include the interactions between fillers and polymers in blends[38] [eq. (4)]. Premphet and Horanont[39] have shown that in filled blends the filler is selectively situated in the polymer phase with which it has the lowest interfacial tension. Sumita et al.[37] introduced a value, ωa, (Table III) for the prediction of the filler localization in either of the polymer phases A (PLA) or B (LDPE), or at the interface between the PLA and LDPE polymers:

$$\omega a = \frac{\gamma_{\text{filler-B}} - \gamma_{\text{filler-A}}}{\gamma_{\text{A-B}}} \quad (4)$$

If $\omega a > 1$, the filler is distributed within phase A (PLA), if $-1 < \omega a < 1$ the filler is located at the interface, and if $\omega a < -1$, the filler is located within phase B (LDPE) (Table III).

The examples of theoretical calculations of ωa have in the literature[40] been used to predict the thermodynamically balanced distribution of nanofillers in a polymer blend.[41,42] In a previous study, we found that nanofillers could act as compatibilizers for blends, but only in the case when they were situated at the interface.[20] The calculation of the thermodynamically preferential filler location in the blend, ωa (Table III), indicated that the SiO_2 nanofillers were situated at the interface. This was characterized by a relatively lower interfacial energy with both the PLA and LDPE polymer components. Besides, silica fillers have very high active surface areas and the commercial pretreatment with silane may additionally activate their surface. On the contrary, the $CaCO_3$ nanofillers, which create an unstable high interfacial energy with both PLA and LDPE phases, were according to calculation positioned in the LDPE phase of the blend rather than at the interface (Table III). The calculation of the interfacial energy, as well as the thermodynamically optimal situation when the fillers are forced to the interface, is based on the measured values of surface energy for a given blend.

It should be mentioned that it is difficult to achieve the exclusive localization of nanofillers at the interface.[43,44] Other factors, such as the efficacy of mixing, viscosity and melt rheology,[45,46] blend composition, and nanofiller agglomeration, could

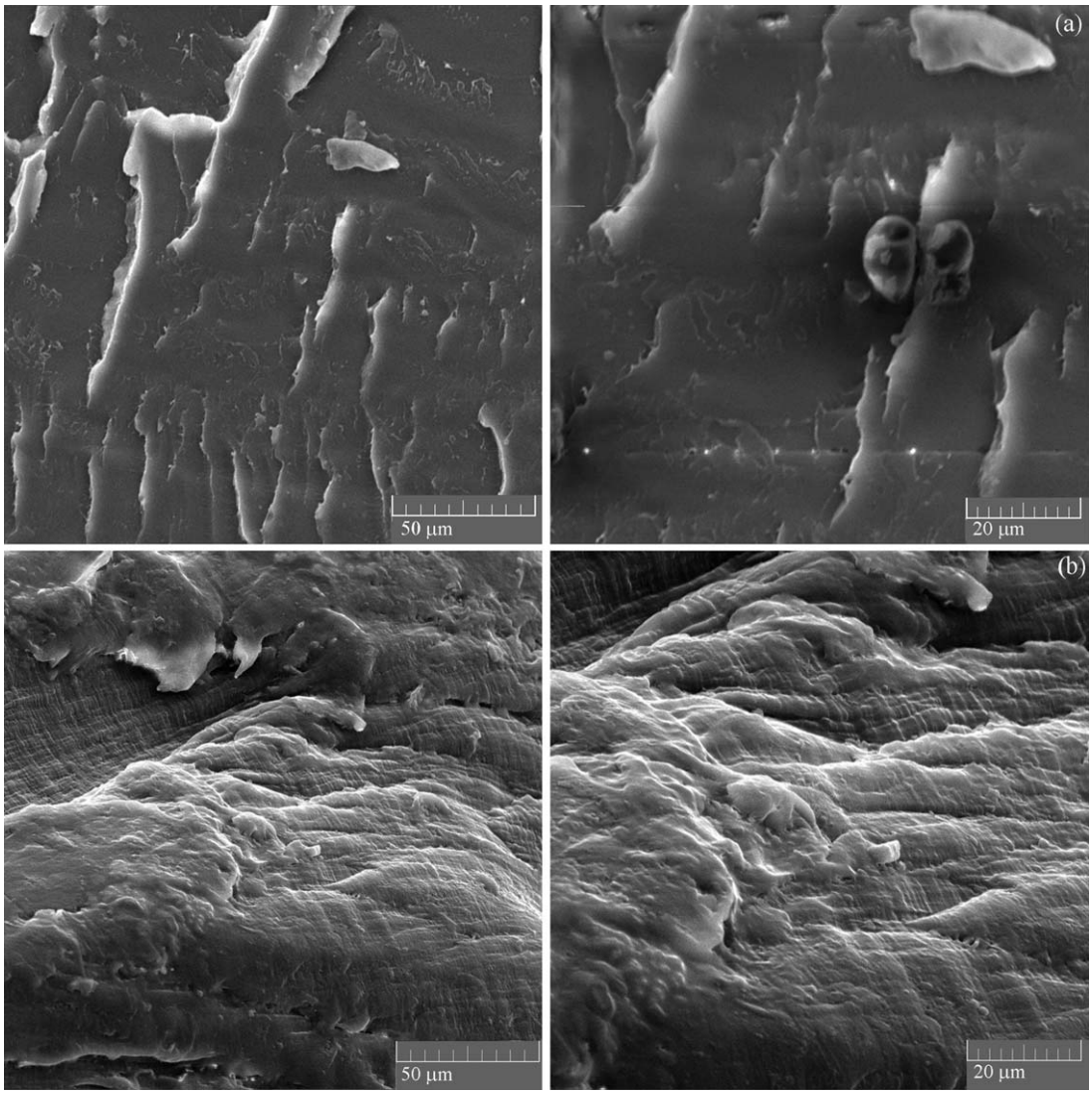

Figure 1. SEM micrographs of fracture surfaces after the failure of pure PLA (a) and LDPE (b).

diminish or even cancel the thermodynamical balance. Only if the other above-mentioned factors are optimized for the selected blend, the nanofillers might act as potential compatibilizers when situated at the interface. In such a case, an improvement of the morphology and properties of a given blend in comparison with the unfilled immiscible blend is expected. The morphology might give more information about the filler effect in PLA/LDPE blends.

Morphology

SEM micrographs of the fracture surfaces for the initial polymer components PLA and LDPE were first analyzed to determine the mechanisms of failure in the pure polymer matrices (Figure 1). Figure 1(a) displays brittle fracture surfaces with little plastic deformation portraying a few long threads of deformed PLA material, which was similar to results found in the literature.[28] Moreover, there was a lack of large-scale plastic deformation.[14]

Conversely, the pure LDPE illustrated in Figure 1(b) presented the behavior of a plastically deformed material. Polymer materials yield when crazing or shear-yielding occurs. The fracture surface of crazing often appears more brittle than that of shear-yielding in the sense that less plastic deformation can be detected on it.[47]

SEM micrographs of unfilled PLA/LDPE blend speciments with various compositions (taken after the tensile tests) are presented in Figure 2. As can be seen, the PLA and LDPE phases were incompatible, that is, they created two distinct phases. Spherical domains of dispersed phases are more commonly formed in systems where phase separation occurs while the polymers are liquid.[48] The sample fracture path follows the particle–matrix interface and holes remain where particles have been pulled out of the matrix polymer, showing weak adhesion between the phases. The higher amount of LDPE phase illustrates the increase in plastic deformation with pulled-out fibrils [Figure 2(b,c)]. The micrographs indicate a weak interfacial adhesion associated with the incompatibility in the PLA/LDPE blend, which corresponds to the negative wetting coefficient shown in Table III. The addition of nanofillers in composites might improve the interactions at the interface with polymer matrix

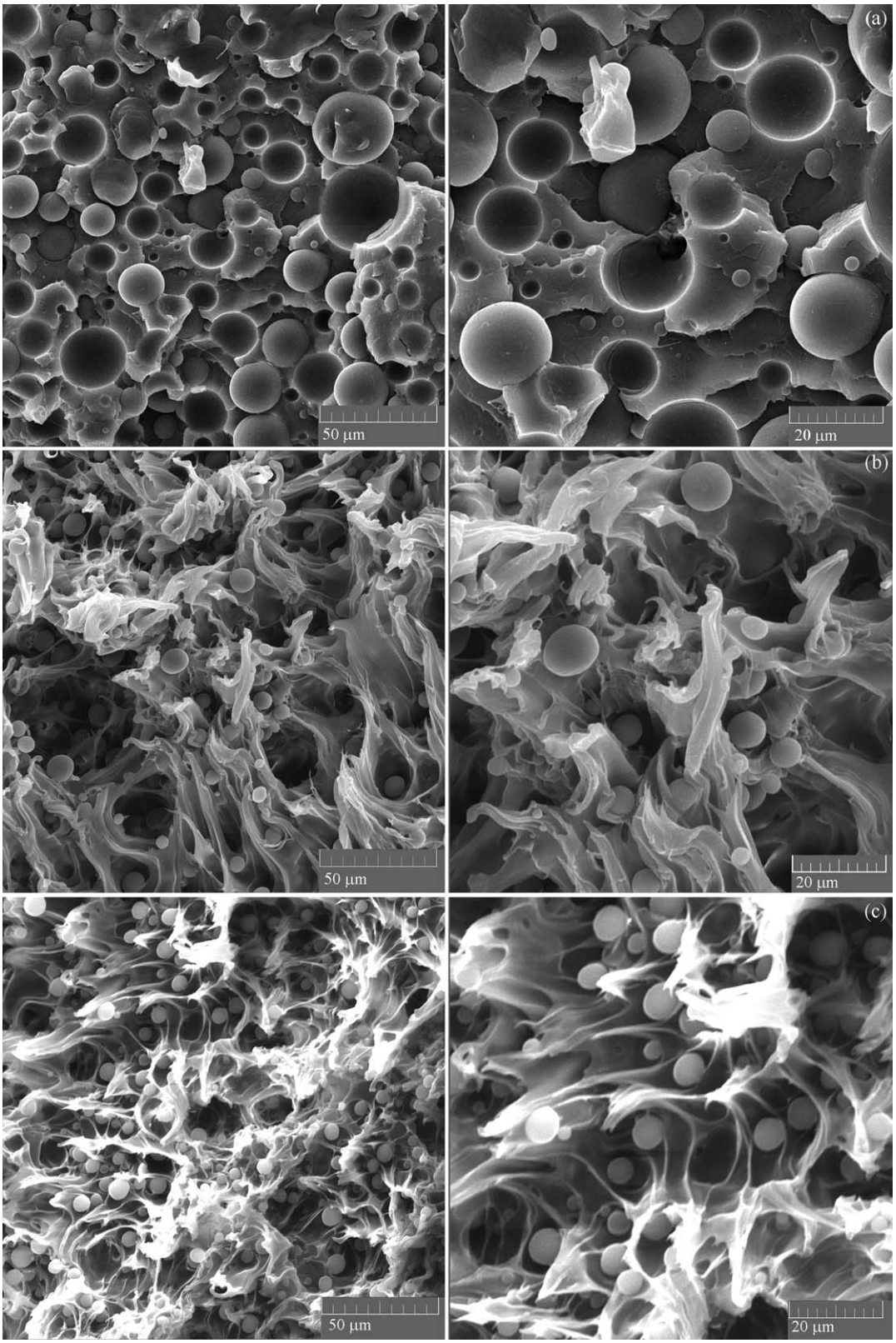

Figure 2. SEM micrographs of unfilled blends of PLA/LDPE 80/20 (a), 50/50 (b), and 20/80 (c).

and reinforce the system. The effect of adding SiO_2 and/or $CaCO_3$ (5 wt %) nanofillers in the pure PLA and LDPE polymers can be seen in Figure 3. The SEM analysis was expected to provide a qualitative view of the bonding process and the nature of the region of the modified matrix surrounding the filler.[48]

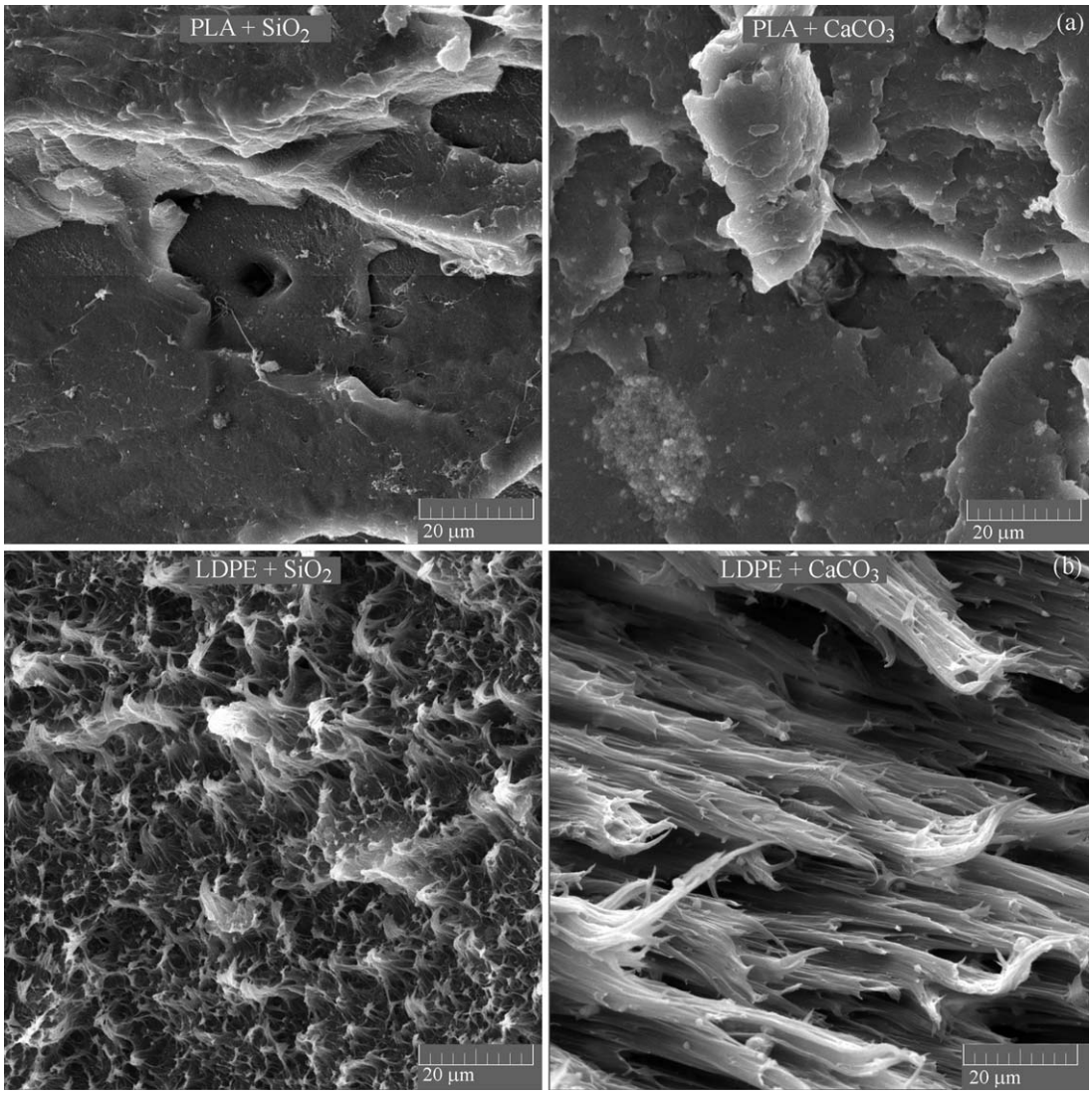

Figure 3. The effects of the SiO_2 and $CaCO_3$ nanofillers (5 wt %) in pure PLA (a) and pure LDPE (b).

The imaging of the PLA/filler composites in Figure 3(a) reveals a better dispersion and distribution of silica fillers as opposed to their $CaCO_3$ counterparts, for which filler agglomerates were highly visible. According to results from the literature,[35] the silica filler with a higher surface area in PLA/SiO_2 composites showed a high level of dispersion (<1 μm) and distribution as well as adhesion to the polymer matrix. Also, it has been found[48] that the chemical modification of fillers might change the failure at the interface from adhesive to cohesive. The commercial treatment of SiO_2 nanofillers, usually with a silane coupling agent, as in our case with methacrylsilane (Table II), promotes the interfacial attraction between the organic PLA phase and the inorganic filler phase and increases the phase compatibility. In some cases, this is due to the covalent bonds through chemical reactions with hydroxyl groups in the organic phase.[17] PLA is known to have slightly polar oxygen atoms which could form hydrogen bonds with hydroxyl groups[49] on filler surfaces and/or produced by the filler pretreatment. Dimple patterns, like those seen in Figure 3(a), have already been found in semicrystalline polymers and are attributed to a fracture of strained craze fibrils.[50] Conversely, the LDPE/filler nanocomposites [Figure 3(b)] showed a larger plastic deformation, especially in the case of LDPE/$CaCO_3$, as a consequence of stress-whitening and necking during tension, with numerous fibrils drawn out of the polymer with cavities residing among them. These cavities are microvoids that initiate a ligament shear-yielding process during tension formed at the polymer/filler interface due to debonding or in the polymer matrix due to the microvoiding of the matrix.[14]

The results in Figure 3 point at the fact that SiO_2 is better distributed in both matrices, that is, PLA and LDPE, than the $CaCO_3$ nanofiller. This is in correlation with the significantly lower energy with both PLA and LDPE matrices, and a more stable interface, contrary to $CaCO_3$ that creates an unstable interface with a much higher interfacial energy as indicated in Table III. The effects of the SiO_2 and $CaCO_3$ fillers on the morphology of the selected filled blend PLA/LDPE/filler (80/20/5)

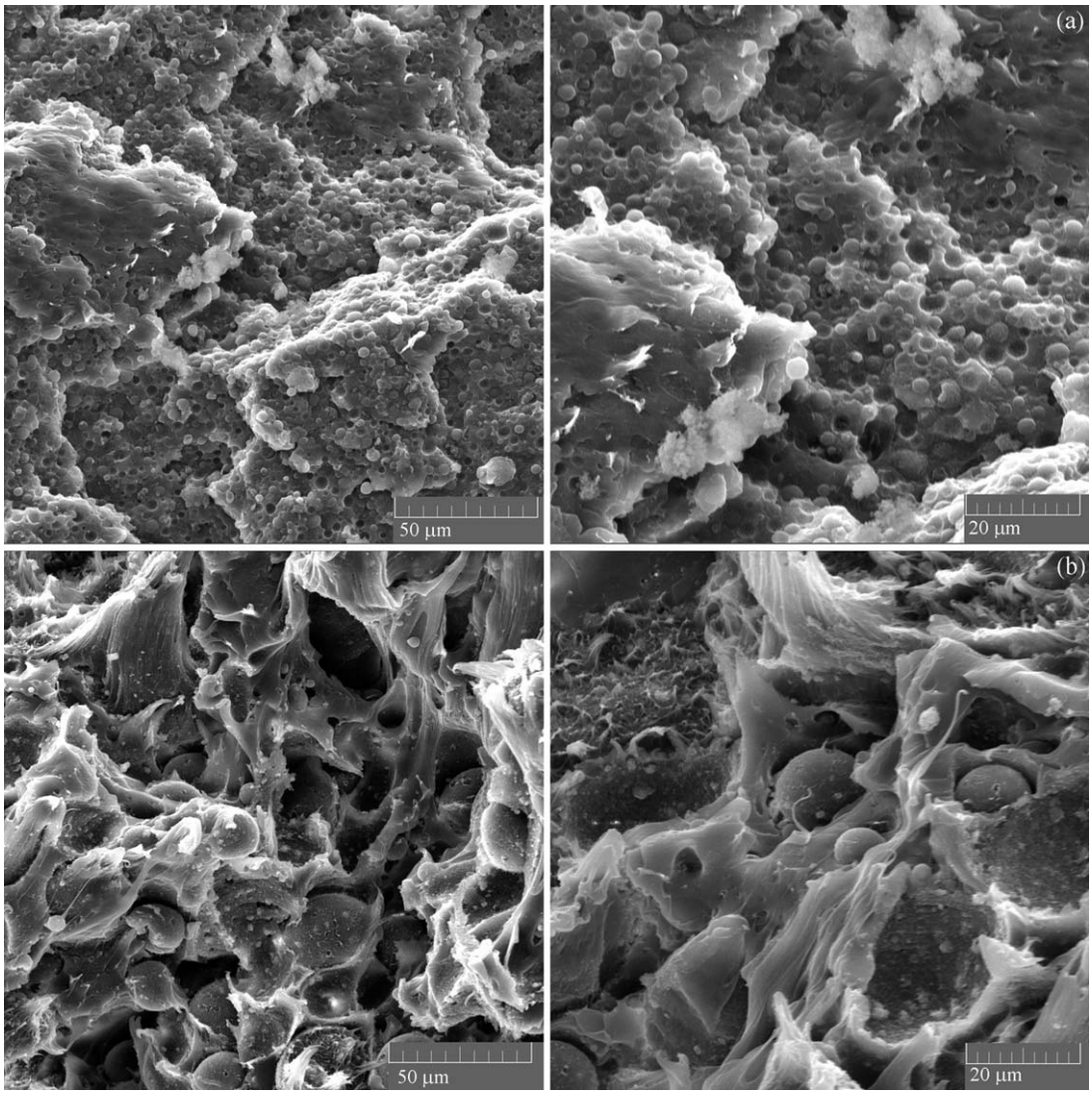

Figure 4. The morphology of PLA/LDPE/filler blends (80/20/5) filled with SiO_2 (a) and $CaCO_3$ (b).

are illustrated in Figure 4. The role of a compatibilizer, for example, a well-designed block copolymer,[51] is to produce a much finer and more uniform phase structure, similar to the results of introducing other compatibilizers into incompatible polymer blends.[52]

It is known from literature that a small amount of nanofiller significantly changes the morphology and lowers the size of dispersed domains in blends.[53,54] Inorganic nanofillers are often added into blends as a third component to modify their performance.[18] It is especially important to clarify the role of interface-localized nanoparticles when determining the properties of polymer blends.[18] When nanofiller particles are thermodynamically forced to the interface, they might surround the dispersed domains in the blend creating a so-called "soft core-rigid shell" structure and "sea-island" morphology.[18]

The morphology of the tensile-fractured surface of the ternary blend PLA/LDPE/SiO_2 (80/20/5) [Figure 4(a)] was much improved in comparison with the unfilled binary blend [PLA/LDPE: 80/20 in Figure 2(a)] with a significant decrease of the dispersed phase size (from ~8–12 μm to ~2–5 μm) due to an increased adhesion and a lack of signs of debonding at the interface. This has been recognized elsewhere as an indication that the compatibility between phases in the blend was improved.[16] The fine morphology of the filled PLA/LDPE/SiO_2 blend in comparison with the rough morphology of the unfilled PLA/LDPE blend of equivalent composition demonstrates that the selected commercially pretreated SiO_2 filler could improve the compatibility between the PLA and LDPE phases. The untreated hydrophilic silica might lead to microcomposites with agglomerates in the polymer matrix, while the pretreated, less hydrophilic, functionalized silica possibly lowered the size of the filler agglomerates and improved its dispersion.[13] The commercially functionalized nanofiller SiO_2 acted as a compatibilizer in the PLA/LDPE blend and produced a finer morphology [Figure 4(a)]. The improvement was believed to originate from the selective localization of SiO_2 at the interface in the PLA/LDPE blends. This assumption was well supported by the calculations based on the optimal SiO_2 filler surface energy, which indicated that the filler was thermodynamically forced to the

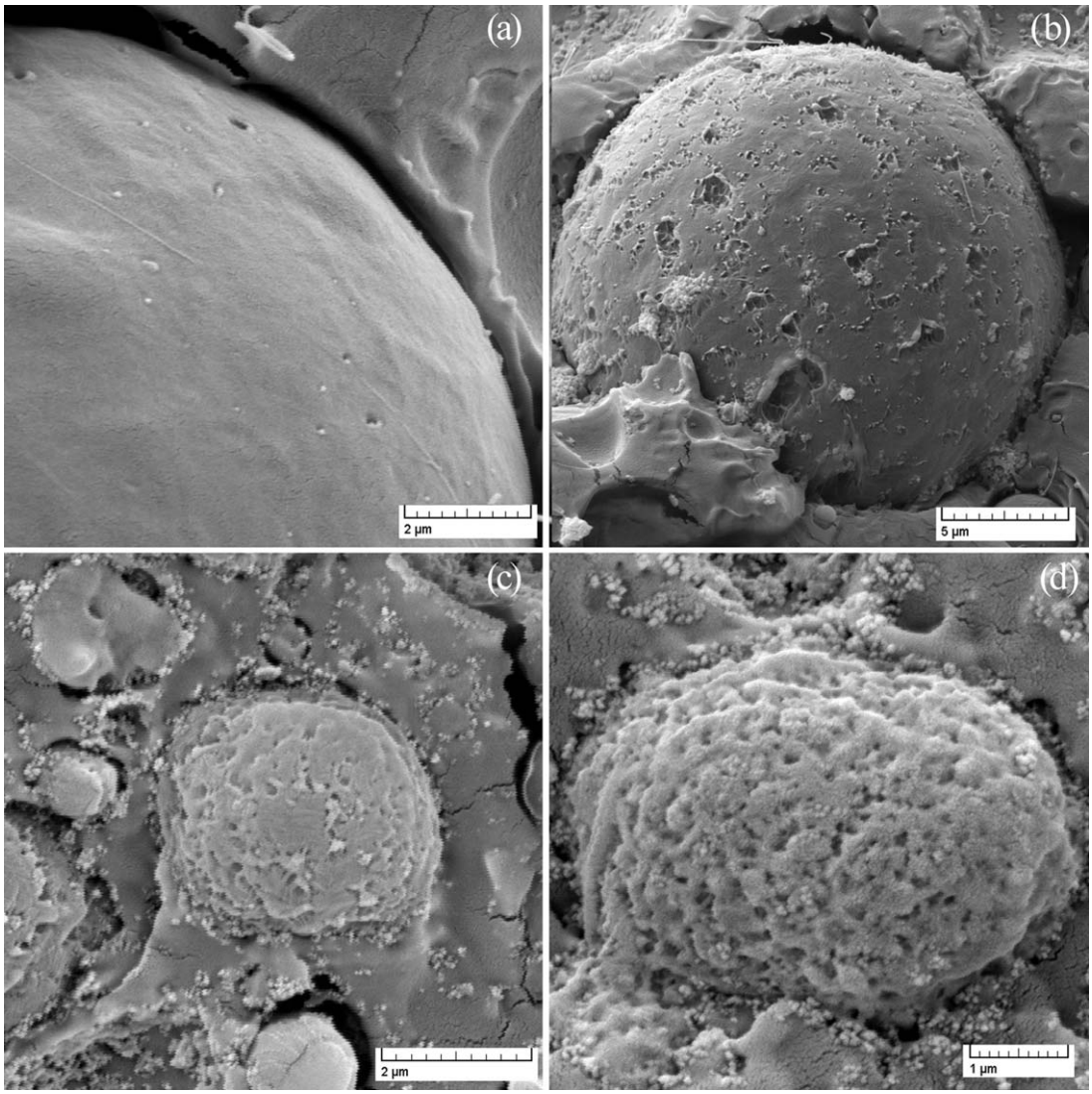

Figure 5. Debonding at the interface of unfilled PLA/LDPE blend (80/20) (a) and in filled blend (80/20/5) with $CaCO_3$ (b) decayed with SiO_2 addition located mostly at the interface (c, d).

interface (Table III). The effect of the efficient compatibilization in the blend[34] is illustrated by the evident matrix deformation, which is characteristic of shear yielding, and the dispersed particles of the other phase not clearly defined by the matrix [Figure 4(a)]. Conversely, the SEM micrograph in Figure 4(b) of the PLA/LDPE 80/20 blend filled with 5 wt % $CaCO_3$ portrays an intensive plastic deformation with no signs of interactions at the interface between phases with a rough fracture surface and visible filler aggregation. Cai at al.[55] confirmed that the morphological evolution of immiscible blends is strongly dominated by self-agglomerating patterns of nanoparticles dispersed in polymer melts. Debonding at the interface in incompatible PLA/LDPE blend (80/20) [Figure 5(a)] is still present in blend with $CaCO_3$ agglomerates (80/20/5) [Figure 5(b)], located mostly in LDPE phase, contrary to the compatibilizing effect of SiO_2 nanofillers [Figure 5(c,d)], visible mostly as coronet situated at the interface (Table III). An increase of the amount of LDPE in the PLA/50LDPE blend worsened the morphology of the unfilled blend but still the addition of SiO_2 lowered the domain size [Figure 6(a)], much more than in the case of $CaCO_3$ filler addition [Figure 6(b)].

Mechanical Properties

The mechanical properties of unfilled PLA/LDPE blends of various compositions are presented in Figure 7 and Table IV. For PLA, the initially high strength at break, as well as its high modulus, was lowered with the addition of LDPE, depending on the composition. Conversely, the high elongation at break of LDPE did not influence the elongation of the blend to any significant extent, except in the case with a higher percentage in the immiscible PLA/LDPE blend. The brittle fracture surfaces of PLA which were visible in SEM micrographs (Figure 1) correlated well with a high modulus and strength at break as well as a very low elongation of the initial PLA. The plastic failure of pure LDPE was followed by a high elongation but a low strength at break (Table IV and Figure 7). The significant drop

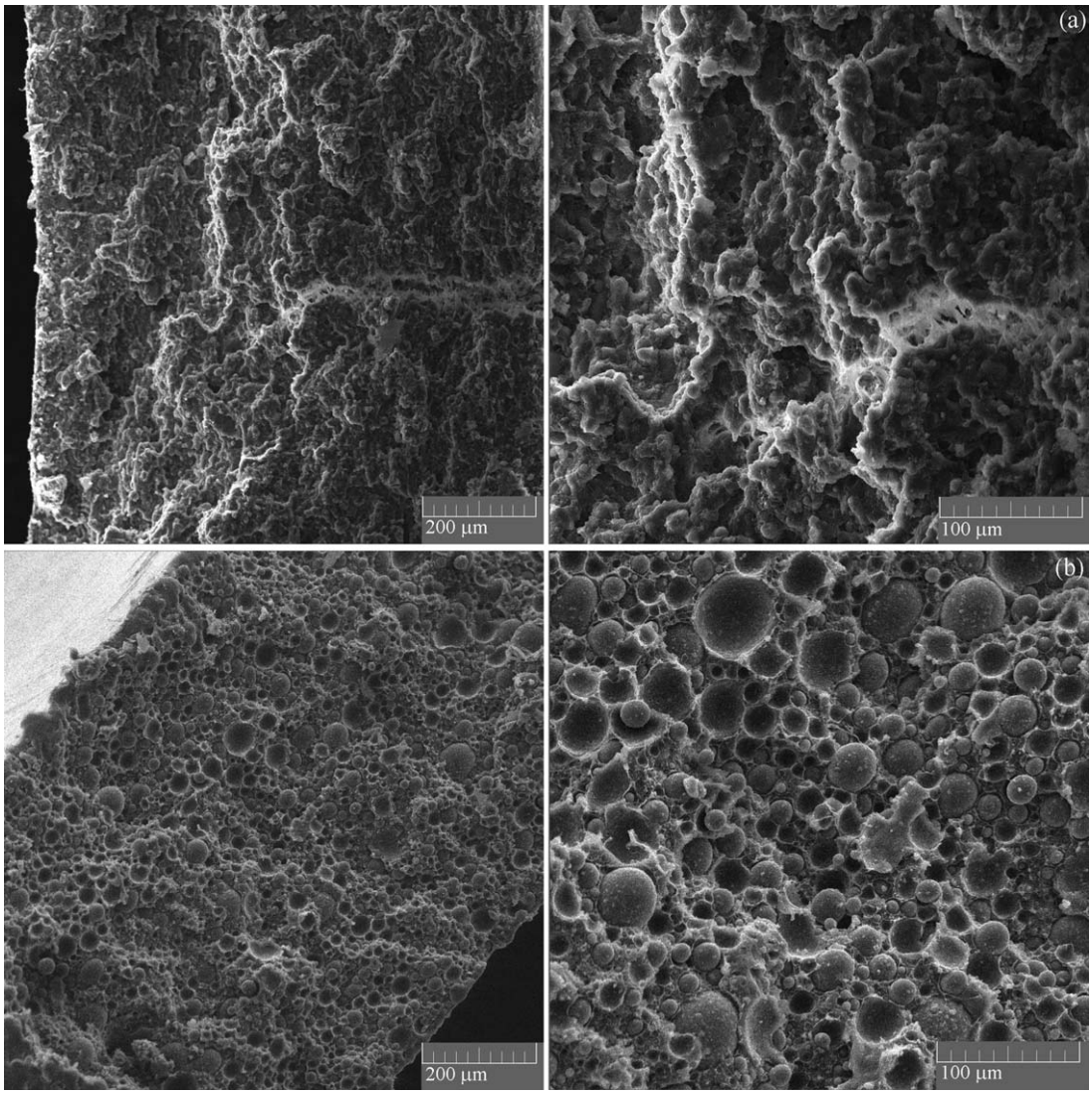

Figure 6. SEM micrographs of filled blends PLA/LDPE (50/50/5) filled with SiO_2 (a) and $CaCO_3$ (b).

in strength at break with the increased amount of LDPE (Table IV) due to a lack of interactions was in agreement with morphological signs of debonding at the interface (Figure 2). This was accompanied by a negative wetting coefficient indicating a debonding of the phases in the PLA/LDPE blend (Table III). It is evident that the failure at the interface appeared due to a lack of adhesion between the phases (Figure 2). Moreover, the significantly increased plastic deformation visible in SEM micrographs [Figure 2(b,c)], lowered the strength as the amount of LDPE was increased in the blend (Table IV). The worsened mechanical properties of the immiscible PLA/LDPE blend as compared with the initial PLA indicated the necessity of using nanofillers as a potential compatibilizer.

The mechanical results of pure PLA and LDPE and selected blends filled with the same percentage (5 wt %) of SiO_2 and/or $CaCO_3$ fillers are presented in Table V. The effect of the SiO_2 nanofiller on the increased strength at break and impact strength in the filled blends in comparison with the unfilled blend (Table IV), especially in the case of a higher amount of PLA, was in correlation with the filler's potential role as a compatibilizer thanks to a lowered interfacial energy (Table III) and being localized at the interface between the PLA and LDPE phases (Figure 5). The initial toughness, measured as the impact strength, showed a slight increase only with the addition of a small amount (10 wt %) of LDPE, and then decreased with

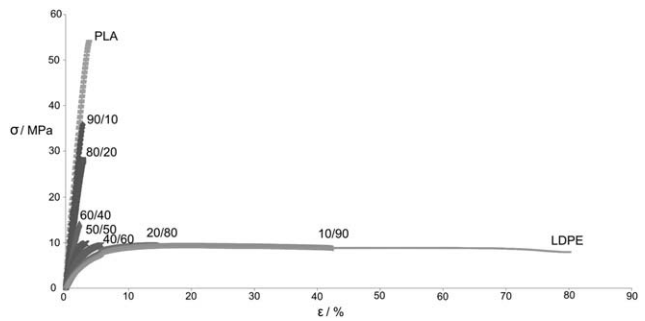

Figure 7. Stress–strain curves of the initial polymers and the PLA/LDPE blends.

Table IV. Mechanical Properties of the Unfilled Blends

Composition (%) PLA/PE-LD	Mechanical properties						
	σ_y (MPa)	ε_y (%)	E (MPa)	σ_b (MPa)	ε_b (%)	W (Nm)	a_{iU} (kJ/m^2)
PLA 100/0	-	-	1496.0	52.9	3.70	0.52	14.2
90/10	-	-	1275.7	34.0	2.68	0.24	16.7
80/20	-	-	906.2	22.8	2.94	0.20	11.8
60/40	-	-	710.5	13.5	2.00	0.07	8.2
50/50	-	-	377.7	8.0	2.82	0.07	9.6
40/60	-	-	272.0	9.1	5.62	0.18	(N)
30/70	-	-	206.8	8.9	7.64	0.22	(N)
20/80	9.9	13.80	192.3	9.4	15.03	0.53	(N)
10/90	9.8	20.05	161.6	8.5	36.53	1.61	(N)
PE-LD 0/100	9.1	17.77	167.0	7.5	64.68	2.80	(N)

(N) = No rupture of the sample occurred during impact.

higher amounts of LDPE (Table IV). The toughness was found to significantly depend on the properties of the dispersed phase in the composites and/or blends. Anderson and Hillmyer[34] reported that the toughness of a blend of poly(L-lactide) (PLLA) and polyethylene could be significantly improved with a PLLA-PE block copolymer as a compatibilizer when the most rigid PE obtained the medium adhesion at the interface. For example, the use of PLA-PE block copolymers as compatibilizers in a blend of PLA with PE changed the interfacial adhesion between the matrix and the dispersed phase depending on the structure of compatibilizer. Wu[56] suggested that the critical distance between the particles of a dispersed (rubbery) phase known as the critical matrix ligament thickness that should be below this value to achieve toughness, where only Van-der-Waals adhesion is necessary to achieve toughness. It is believed that the critical distance is related to the overlay of stress fields around the dispersed phase. When the stress fields interplay, the matrix phase is subjected to shear yielding, which gives rise to a tough behavior.[34] On the contrary, other authors have claimed that an increase in interfacial adhesion is adversative to toughness,[57] and/or has no influence on it.[58]

Our results showed that the addition of a commercial silica nanofiller which was pretreated with methacrylsilane (Table II) increased the toughness, but also the strength, in a PLA/LDPE/SiO_2 blend with a higher amount of PLA (Table V). It is known that the too strong hydrophilic interactions between the untreated silica nanofillers and the matrix caused by Si—OH groups, that is, hydrogen and Van der Waals bonds, might be reduced and optimized by a surface modification of the silica, which in turn increases the fine dispersion of silica in the polymer matrix.[13] Mechanical results in Table V confirmed that the

Table V. Mechanical Properties of the PLA/LDPE Blends Filled with 5 wt % Nanofillers

Composition (%)	Mechanical properties						
	σ_y (MPa)	ε_y (%)	E (MPa)	σ_b (MPa)	ε_b (%)	W (Nm)	a_{iU} (kJ/m^2)
PLA/PE-LD + SiO_2							
PLA 100/0	-	-	1665.4	51.1	3.04	0.33	12.5
90/10	-	-	1372.2	40.9	2.80	0.30	17.7
80/20	-	-	1241.4	34.9	2.68	0.26	17.6
50/50	-	-	342.8	16.5	3.01	0.16	11.0
10/90	10.6	9.29	224.9	10.6	9.52	0.39	(N)
PE-LD 0/100	8.7	8.66	192.2	6.3	11.89	0.46	(N)
PLA/PE-LD + $CaCO_3$							
PLA 100/0	-	-	1785.1	43.3	2.51	0.28	14.3
90/10	-	-	1355.3	33.9	2.39	0.22	14.5
80/20	-	-	1127.4	31.7	2.67	0.22	9.8
50/50	-	-	305.7	9.5	2.60	0.08	7.7
10/90	10.9	11.2	221.3	10.6	11.54	0.63	(N)
PE-LD 0/100	10.0	16.1	178.7	7.6	57.45	2.45	(N)

(N) = During impact there is no rupture of the sample.

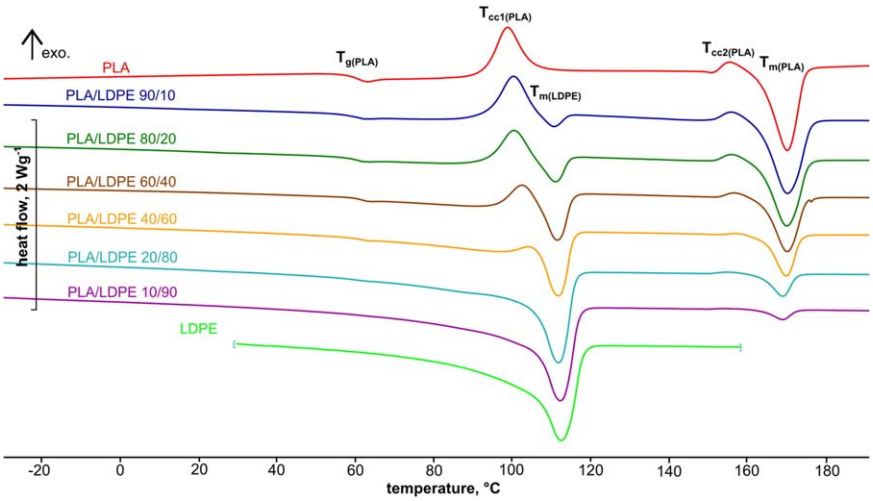

Figure 8. DSC scans of the second heating of the initial PLA, LDPE, and their blends. [Color figure can be viewed in the online issue, which is available at wileyonlinelibrary.com.]

addition of SiO_2 filler which raised the interfacial adhesion between PLA and LDPE, leading to a significant improvement of the strength at break and the toughness. These improvements in mechanical properties of the blends filled with silica correlated well with the observed fine morphology with silica mostly located at the interface, contrary to the effect of the $CaCO_3$ filler (Figures 4 and 5). The addition of $CaCO_3$ nanofillers had a smaller effect on the improvements of the properties in the filled blend, which was in agreement with the results of an unstable high interfacial energy and filler situation in one of the phases (LDPE) rather than at the interface (Table III). The highest impact resistance, together with the highest strength at break, determined by the fine morphology obtained for the blend composition PLA/10–20LDPE/5SiO_2 (Table V), was a result of an optimal composition and the efficacy of SiO_2 as a compatibilizer.

Thermal Properties and Crystallinity

In order for biopolymers to compete with the commodity plastics, their mechanical properties should be at least equivalent or better. Improved mechanical properties of the biopolymer PLA may be achieved by the addition of silica nanofillers that created nanostructures and increased the crystallinity due to the effect as a nucleating agent for PLA's crystallization.[13] The tensile properties of PLA may also vary depending on its crystallinity.[59] DSC measurements were thus performed to determine the thermal properties and potential PLA crystallinity in unfilled and filled PLA/LDPE blends. DSC thermograms of the second heating of the initial PLA, LDPE, and their blends with various compositions are presented in Figure 8 and Table VI. The degree of crystallinity for PLA can be seen in Table VI and was calculated using eq. (3). It depends on the molecular architecture and thermal history of the sample.[28] The DSC

Table VI. Thermal Characteristics of PLA, LDPE, and PLA/LDPE Blends with the Calculated Degree of Crystallinity for PLA

Samples	Glass transition	Cold crystallization PLA				Melting LDPE		Melting PLA		PLA degree of crystall[a]
PLA/PELD	T_g (°C)	T_{cc1} (°C)	ΔH_{cc1} (J/g)	T_{cc2} (°C)	ΔH_{cc2} (J/g)	T_{mPELD} (°C)	ΔH_{mPELD} (J/g)	T_{mPLA} (°C)	ΔH_{mPLA} (J/g)	χ_{cPLA} (%)
PLA										
100/0	59.4	98.9	24.7	155.0	3.3	-	-	169.9	35.5	38.1
90/10	59.1	100.4	19.5	155.8	2.8	110.6	3.2	169.9	37.4	44.6
80/20	59.6	100.4	16.9	155.8	2.3	111.1	5.8	169.8	31.4	42.2
60/40	61.3	102.6	9.2	156.6	1.3	111.8	11.9	170.0	23.9	42.8
40/60	60.2	104.3	2.4	156.9	0.6	111.9	16.1	169.6	15.1	40.5
20/80	-	-	-	-	-	111.8	80.4	168.8	7.9	42.4
10/90	-	-	-	-	-	112.3	91.3	168.7	3.5	37.6
PELD										
0/100	-	-	-	-	-	112.8	102.5	-	-	-

[a] χ_c [eq. (3)].

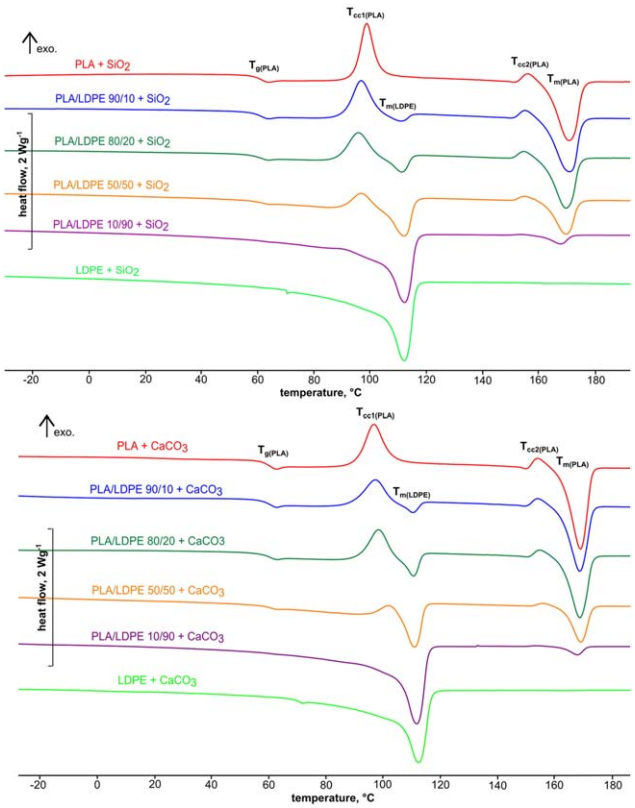

Figure 9. DSC thermograms of the second heating of samples filled with 5 wt % of SiO_2 (a) and $CaCO_3$ (b). [Color figure can be viewed in the online issue, which is available at wileyonlinelibrary.com.]

thermograms in Figure 8 and the data in Table VI illustrate the clear glass transition of the initial PLA at $T_g = 59.4°C$ and two peaks of cold crystallization at $T_{cc1} = 98.9°C$ and $T_{cc2} = 155.0°C$ with a large melting peak at $T_m = 169.9°C$. Two crystallization peaks for PLA were described by Hoogsteen et al.,[60] and assigned to the two crystalline modifications, that is, orthorhombic (β) and pseudo-ortorombic (α) structures. The relative degree of crystallinity in the PLA/LDPE blend was calculated from the enthalpy of fusion while the first PLA peak at ~100°C, corresponding to cold crystallization, became overlapped by the LDPE melting peak at ~110°C as the LDPE phase increased. The second small crystallization peak, visible in Figure 8 at ~155°C, just before the PLA melting, disappeared when the amount of LDPE was increased. Polylactide can crystallize if it is annealed above T_g and the degree of crystallinity and the melting point may vary although they depend significantly on annealing, conditions of polymerization, and amount of *meso*-, D-, or L-lactide.[61] The melting temperature and degree of PLA crystallinity generally depend on the molecular mass, thermal history, and purity of the polymer.[62,63] The commercially available PLA is usually a copolymer of poly(L-lactide) with *meso*-lactides or D-lactides, where the content of D-enantiomers influences the PLA properties such as the melting temperature, degree of crystallinity, and so forth.[2] The crystallinity is usually lower with a higher content of L-isomer, and the same goes for the glass transition temperature and melting temperature.[64,65] Depending on the amount of optically active L- in D,L-enantiomers, which usually constitute commercial PLA,[31] PLA can crystallize in three forms (α, β, and γ). The α-structure is more stable and has a melting point $T_{m\alpha} = 185°C$ that is higher than that of the β-structure, that is, $T_{m\beta} = 175°C$.[6] With the reduction in

Table VII. DSC Analysis of the Binary and Ternary PLA/LDPE Blend Compositions

Samples	Glass transition T_g (°C)	PLA cold crystallization T_{cc} (°C)	PLA cold crystallization ΔH_{cc} (J/g)	LDPE melting $T_{mPE\text{-}LD}$ (°C)	LDPE melting $\Delta H_{mPE\text{-}LD}$ (J/g)	PLA melting T_{mPLA} (°C)	PLA melting ΔH_{mPLA} (J/g)	PLA degree of crystall.[a] χ_{PLA} (%)
PLA/PE-LD +5 wt % SiO_2								
100/0	61.0	98.7	29.4	-	-	170.9	44.6	47.9
90/10	60.7	96.6	24.8	111.0	3.8	171.0	40.7	51.1
80/20	60.6	95.8	22.3	111.3	7.2	169.8	34.7	49.0
50/50	61.3	97.0	14.4	112.5	16.6	169.7	22.4	50.7
10/90	-	-	-	112.3	81.4	167.8	4.1	46.7
0/100	-	-	-	112.1	100.4	-	-	-
PLA/PE-LD +5 wt % $CaCO_3$								
PLA 100/0	59.9	96.8	28.8	-	-	169.1	46.9	50.4
90/10	60.0	97.3	14.5	110.4	5.6	168.8	39.2	49.2
80/20	60.5	98.6	15.5	110.9	10.6	169.2	37.0	52.2
50/50	60.3	101.6	2.5	110.9	19.6	169.1	20.1	45.5
10/90	-	-	-	111.8	92.5	168.0	4.1	45.8
0/100	-	-	-	112.5	113.0	-	-	-

[a] χ_c [eq. (3)].

content of L-isomers, a lowering of the crystallinity, as well as of T_m and T_g, was observed.[64,65] The presence of meso-lactides can lower T_m by 50°C.[31] The increased amount of LDPE in the blend did not change T_m, T_g, or the initial degree of crystallinity. The enthalpies of melting and crystallization were significantly reduced with the higher amount of LDPE in the PLA/LDPE blend (Table VI), which was expected due to the lower mass content of PLA.

The effects of filler addition on the DSC thermograms are visible in Figure 9 and Table VII. The crystallinity of the pure PLA matrix, as well as of the filled blends (Table VI), increased with addition of either of the nanofillers (i.e., SiO_2 or $CaCO_3$) (Table VII). The resultant higher crystallinity might be a consequence of a favored nucleation[66] and regular arrangement of PLA chains.[19]

CONCLUSIONS

The surface energy investigations of the given components in PLA/LDPE/nanofiller blends and the calculation of thermodynamic parameters at the interface were used as an indication of the potential role of a nanofiller as a compatibilizer in conditions where it is preferentialy situated at the interface.

The commercially pretreated SiO_2 nanofiller, which according to the thermodynamical calculations and morphology proofs was mostly located at the interface, acted as a compatibilizer in the PLA/LDPE blend, as it significantly lowered the size of the dispersed domains and thus improved the dispersion and interactions, correspondingly enhancing the mechanical properties of the filled blend.

The commercial $CaCO_3$ nanofiller showed less efficacy, which in the PLA/LDPE blend caused a failure of the heterogeneous surface with signs of phase debonding followed by visible plastic deformations that lowered the strength at break of the incompatible systems. This was in correlation with the high interfacial energy and preferential filler localization in one of the phases (LDPE) rather than at the interface.

The decreased size of the dispersed domains and the fine morphology in the PLA/LDPE/SiO_2 blend demonstrated that SiO_2 could improve the compatibility between the PLA and LDPE phases, and as a consequence increase the toughness and crystallinity of the final material.

ACKNOWLEDGMENTS

This study was supported by the Ministry of Science, Education and Sports of the Republic of Croatia (grant number 125-1252971-2575).

REFERENCES

1. Jamshidian, M.; Tehrany, E. A.; Imran, M.; Jacquot, M.; Desorby, S. *Compr. Rev. Food Sci. Food Saf.* **2010**, *9*, 552.
2. Sinha Ray, S.; Okamoto, M. *Macromol. Rapid Commun.* **2003**, *24*, 815.
3. Rezgui, F.; Swistek, M.; Hiver, J. M.; Sell, C. G.; Sadoun, T. *Polymer* **2005**, *46*, 7370.
4. Chen, C.-C.; Chueh, J.-Y.; Tseng, H.; Huang, H.-M.; Lee, S.-Y. *Biomaterials* **2003**, *24*, 1167.
5. Madhavan Nampoothiri, K.; Rajendran Nair, N.; Pappy John, R. *Bioresource Technol.* **2010**, *101*, 8493.
6. Auras, R.; Harte, B.; Selke, S. *Macromol. Biosci.* **2004**, *4*, 835.
7. Ochi, S. *Mech. Mater.* **2008**, *40*, 446.
8. Gottschalk, C.; Frey, H. *Macromolecules* **2006**, *39*, 1719.
9. Schugens, Ch.; Grandfils, Ch.; Jerome, R.; Teyssie, Ph.; Delree, P.; Martin, D.; Malgrange, B.; Moonen, G. *J. Biomed. Mater. Res.* **1995**, *29*, 1349.
10. Drumright, R. E.; Gruber, P. R.; Henton, D. E. *Adv. Mater.* **2000**, *12*, 1841.
11. Davis, G.; Song, J. H. *Ind. Crops Prod.* **2006**, *23*, 147.
12. Lotti, M.; Fabbri, P.; Messori, M.; Pilati, F.; Fava, P. *J. Polym. Environ.* **2009**, *17*, 10.
13. Prébé, A.; Alcouffe, P.; Cassagnau, Ph.; Gerard, J. F. *Mater. Chem. Phys.* **2010**, *124*, 399.
14. Jiang, L.; Zhang, J.; Wolcott, M. P. *Polymer* **2007**, *48*, 7632.
15. Park, J. W.; Im, S. S. *Polymer* **2003**, *44*, 4341.
16. Yao, M.; Deng, H.; Mai, F.; Wang, K.; Zhang, Q.; Chen, F.; Fu, Q. *eXPRESS Polym. Lett.* **2011**, *5*, 937.
17. Bang, G.; Woo Kim, S. *J. Ind. Eng. Chem.* **2012**, *18*, 1063.
18. Xiu, H.; Bai, H. W.; Huang, C. M.; Xu, C. L.; Li, X. Y.; Fu, Q. *eXPRESS Polym. Lett.* **2013**, *7*, 261.
19. Fortunati, E.; Armentano, I.; Iannoni, A.; Kenny, J. M. *Polym. Degrad. Stabil.* **2010**, *95*, 2200.
20. Hrnjak-Murgić, Z.; Jelčić, Ž.; Kovačević, V.; Mlinac-Mišak, M.; Jelenčić, J. *Macromol. Mater. Eng.* **2002**, *287*, 684.
21. Vrsaljko, D.; Leskovac, M.; Lučić Blagojević, S.; Kovačević, V. *Polym. Eng. Sci.* **2008**, *48*, 1931.
22. Kratofil Krehula, L. J.; Ptiček Siročić, A.; Katančić, Z.; Jelenčić, J.; Kovačević, V.; Hrnjak-Murgić, Z. *J. Appl. Polym. Sci.* **2012**, *126*, 1257.
23. Zhang, Q.; Yang, H.; Fu, Q. *Polymer* **2004**, *45*, 1913.
24. Fenouillot, F.; Cassagnau, P.; Majesté, J.-C. *Polymer* **2009**, *50*, 1333.
25. Comyn, J. *Int. J. Adhes. Adhes.* **1992**, *12*, 145.
26. Wu, S. Polymer Interface and Adhesion; Marcel Dekker: New York, **1982**.
27. Wu, S. *J. Adhes.* **1973**, *5*, 9.
28. Kulinski, Z.; Piorkowska, E. *Polymer* **2005**, *46*, 10290.
29. Si, M.; Araki, T.; Ade, H.; Kilcoyne, A. L. D.; Fisher, R.; Sokolov, J. C.; Rafailovich, M. H. *Macromolecules* **2006**, *39*, 4793.
30. Riga, A.; Zhang, J.; Collis, J. *J. Therm. Anal. Calorim.* **2004**, *75*, 257.
31. Lim, T.; Auras, R.; Rubino, M. *Prog. Polym. Sci.* **2008**, *33*, 820.
32. Liu, H.; Chen, F.; Liu, B.; Estep, G.; Zhang, J. *Macromolecules* **2010**, *43*, 6058.
33. Liu, H.; Song, W.; Chen, F.; Guo, L.; Zhang, J. *Macromolecules* **2011**, *44*, 1513.

34. Anderson, K. S.; Hillmyer, M. A. *Polymer* **2004**, *45*, 8809.
35. Fukushima, K.; Tabuani, D.; Abbate, C.; Arena, M.; Rizzarelli, P. *Eur. Polym. J.* **2011**, *47*, 139.
36. Kovačević, V.; Vrsaljko, D.; Lučić Blagojević, S.; Leskovac, M. *Polym. Eng. Sci.* **2008**, *48*, 1994.
37. Sumita, M.; Sakata, K.; Asai, S.; Miyasaka, K.; Nakagawa, H. *Polym. Bull.* **1991**, *25*, 265.
38. Steinmann, S.; Gronski, W.; Friedrich, C. *Polymer* **2002** *43*, 4467.
39. Premphet, K.; Horanont, P. *Polymer* **2000**, *41*, 9283.
40. Bose, S.; Bhattacharyya, A. R.; Kodgire, P. V.; Misra, A. *Polymer* **2007**, *48*, 356.
41. Jancar, J.; Dibenedetto, A. T. *J. Mater. Sci.* **1994**, *29*, 4651.
42. Wu, D.; Sun, Y.; Lin, D.; Zhou, W.; Zhang, M.; Yuan, L. *Macromol. Chem. Phys.* **2011**, *212*, 1700.
43. Wu, D.; Zhang, Y.; Zhang, M.; Yu, W. *Biomacromolecules* **2009**, *10*, 417.
44. Li, W.; Karger-Kocsis, J.; Tomann, R. *J. Polym. Sci. Part B: Polym. Phys.* **2009**, *47*, 1616.
45. Clarke, P.; Clarke, B.; Freakley, P. K.; Sutherland, I. *Plast. Rubber Compos.* **2001**, *30*, 39.
46. Meijer, H. E. H.; Janssen, J. M. H. In Mixing and Compounding of Polymers; Manas-Zloczower, I.; Tadmor, T., Eds.; Carl Hanser Verlag: Munich, **1994**, p 85.
47. Anderson, T. L. Fracture Mechanics, 2nd ed.; CRC Press: Boca Raton, **1995**, p 34, 322.
48. Sawyer, L. C.; Grubb, D. T. Polymer microscopy; Chapman & Hall: London, 1996, p 233, 257, 259.
49. Bax, B.; Müssig, J. *Compos. Sci. Technol.* **2008**, *68*, 1601.
50. Narisawa, I.; Ishikawa, M. *Adv. Polym. Sci.* **1990**, *91/92*, 353.
51. Chen, B.; Li, X.; Xu, S.; Tg, T.; Zhou, B.; Huang, B. *Polymer* **2002**, *43*, 953.
52. Gao, J.; Bai, H.; Zhang, Q.; Gao, Y.; Chen, L.; Fu, Q. *eXPRESS Polym. Lett.* **2012**, *6*, 860.
53. Hong, J. S.; Namkung, H.; Ahn, K. H.; Lee, J. S.; Kim, C. Y. *Polymer* **2006**, *47*, 3967.
54. Gubbels, F.; Jerome, R.; Teyssie, Ph.; Vanlathem, E.; Deltour, R.; Calderone, A.; Parente, V.; Bredas, J. L. *Macromolecules* **1994**, *27*, 1972.
55. Cai, X.; Li, B.; Pan, Y.; Wu, G. *Polymer* **2012**, *53*, 259.
56. Wu, S. *J. Appl. Polym. Sci.* **1988**, *35*, 549.
57. Liu, Z.; Zhu, X.; Wu, L.; Li, Y.; Qi, Z.; Choy, C.; Wang, F. *Polymer* **2001**, *42*, 737.
58. Borggreve, R. J. M.; Gaymans, R. *J. Polymer* **1995**, *36*, 921.
59. Garlotta, D. *J. Polym. Environ.* **2002**, *9*, 63.
60. Hoogsteen, W.; Postema, A. R.; Pennings, A. J.; Brinke, T.; Zugenmaier, P. *Macromolecules* **1990**, *23*, 634.
61. Hartmann, M. H. In Biopolymers from Renewable Resources; Kaplan, D. L., Ed.; Springer-Verlag: Berlin, **1998**, p 367.
62. Jamshidi, K.; Hyon, S-H.; Ikada, Y. *Polymer* **1988**, *29*, 2229.
63. Migliaresi, C.; De Lollis, A.; Fambri, L.; Cohn, D. *Clin. Mater.* **1991**, *8*, 111.
64. Urayama, H.; Moon, S. I.; Kimura, Y. *Macromol. Mater. Eng.* **2003**, *288*, 137.
65. Dorgan, J. R.; Jansen, J.; Clayton, M. P. *J. Rheol.* **2005**, *49*, 607.
66. Lei Wu, C.; Qui Zhang, M.; Zhi Rong, M.; Friedrich, K. *Compos. Sci. Technol.* **2005**, *65*, 635.